process elucidates a correlation with the $b \to c\ell\nu$ process. The operator responsible for the the $b \to c\ell\nu$ transition can also generate the $b \to s\ell\ell$ and $b \to s\nu\nu$ transitions. This implies the constraints from $b \to s\ell\ell$ and $b \to s\nu\nu$ processes shall also be subject to the bounds from $b \to c\ell\nu$ process. We explore various observables associated with the aforementioned decay modes such as differential branching ratio (DBR), forward-backward asymmetry (A_{FB}^{τ}), and lepton flavor universality parameter (R_{Ξ_b}) within the SM and the presence of SMEFT NP operators.

2 Theoretical Framework

2.1 General Effective Hamiltonian

Dimension six SMEFT lagrangian can be expressed as [6]

$$\mathcal{L}_{\text{eff}} = \mathcal{L}_{\text{SM}} + \sum_{Q_i = Q_i^\dagger} \frac{C_i}{\Lambda^2} Q_i + \sum_{Q_i \neq Q_i^\dagger} \left(\frac{C_i}{\Lambda^2} Q_i + \frac{C_i^*}{\Lambda^2} Q_i^\dagger \right). \tag{1}$$

In the SMEFT, the operators which will be relevant for the $b \to c(u)\ell^-\bar{\nu}_\ell$ transitions are given as [6],

$$\begin{aligned}
Q_{\ell q}^{(3)} &= (\bar{\ell}_i \gamma_\mu \tau^I \ell_j)(\bar{q}_k \gamma^\mu \tau^I q_l), \qquad Q_{\phi ud} = i(\tilde{\phi}^\dagger D_\mu \phi)(\bar{u}_i \gamma^\mu d_j), \\
Q_{\ell edq} &= (\bar{\ell}_i^a e_j)(\bar{d}_k q_l^a), \qquad\qquad Q_{\ell equ}^{(1)} = (\bar{\ell}_i^a e_j)\epsilon_{ab}(\bar{q}_k^b u_l), \\
Q_{\ell equ}^{(3)} &= (\bar{\ell}_i^a \sigma^{\mu\nu} e_j)\epsilon_{ab}(\bar{q}_k^b \sigma_{\mu\nu} u_l), \quad Q_{\phi q}^{(3)} = (\phi^\dagger i \overleftrightarrow{D}_\mu \phi)(\bar{q}_i \tau^I \gamma^\mu q_j).
\end{aligned} \tag{2}$$

In the above equation, ℓ, q and ϕ represent lepton, quark and Higgs $SU(2)_L$ doublets, while the right-handed isospin singlets are denoted by e, u and d. Due to $SU(2)_L$ relations the operators $Q_{\ell q}^{(3)}$, $Q_{\phi q}^{(3)}$ enter the leptonic and semileptonic B decays with underlying quark level transitions $b \to s\ell\ell$ and $b \to s\nu\nu$.

In the presence of SMEFT NP the WET operators get modified and can be expressed as follows [6]

$$\begin{aligned}
C_{V_L} &= -\frac{v^2}{\Lambda^2}\frac{V_{cs}}{V_{cb}}(C_{\ell q}^{(3)ll23} - C_{\phi q}^{(3)23}), \qquad C_{V_R} = \frac{v^2}{2\Lambda^2 V_{cb}} C_{\phi ud}^{23}, \\
C_{S_L} &= -\frac{v^2}{2\Lambda^2}\frac{V_{cs}}{V_{cb}} C_{\ell edq}^{*ll32}, \qquad\qquad C_{S_R} = -\frac{v^2}{2\Lambda^2}\frac{V_{tb}}{V_{cb}} C_{\ell equ}^{*(1)ll32}, \\
C_T &= -\frac{v^2}{2\Lambda^2}\frac{V_{tb}}{V_{cb}} C_{\ell equ}^{*(3)ll32}.
\end{aligned} \tag{3}$$

2.2 $\Xi_b \to \Xi_c \tau^- \bar{\nu}_\tau$ decay

The double differential decay rate corresponding to the $\Xi_b \to \Xi_c \tau^- \bar{\nu}_\tau$ decay is given as follows [7]

$$\frac{d^2\Gamma}{dq^2\, d\cos\theta} = N\left(1 - \frac{m_l^2}{q^2}\right)^2 \left[\mathcal{A}_1 + \frac{m_l^2}{q^2}\mathcal{A}_2 + 2\mathcal{A}_3 + \frac{4m_l}{\sqrt{q^2}}\mathcal{A}_4\right]. \tag{4}$$

The explicit form of $\mathcal{A}_1$, $\mathcal{A}_2$,$\mathcal{A}_3$, $\mathcal{A}_4$ can be found in the ref [7]. After integrating out with respect to $\cos\theta$ the differential branching ratio is given as

$$\frac{d\Gamma}{dq^2} = \frac{G_F^2 |V_{cb}|^2 q^2 |\vec{P}_{B_2}|}{512\,\pi^3\, m_{B_1}^2}\left(1 - \frac{m_l^2}{q^2}\right)^2 H_{\frac{1}{2}\to\frac{1}{2}}\,, \tag{5}$$

where $H_{\frac{1}{2}\to\frac{1}{2}}$ denote the helicity amplitude containing both SM and NP contributions. The detailed forms of the helicity amplitudes can be found in ref [7]. We also consider the forward-backward asymmetry and ratio of the branching fractions in our analysis which are defined as follows

- **Branching fraction ratio** :

$$R_{\Xi_c}(q^2) = \frac{\frac{d\Gamma}{dq^2}(\Xi_b \to \Xi_c \tau^- \bar{\nu}_\tau)}{\frac{d\Gamma}{dq^2}(\Xi_b \to \Xi_c \ell^- \bar{\nu}_\ell)} \tag{6}$$

- **Forward-backward asymmetry**:

$$A_{FB}^{\tau}(q^2) = \frac{\left(\int_0^1 - \int_1^0\right)\frac{d^2\Gamma}{dq^2 d\cos\theta} d\cos\theta}{\left(\int_0^1 + \int_1^0\right)\frac{d^2\Gamma}{dq^2 d\cos\theta} d\cos\theta}, \tag{7}$$

where $d\Gamma^{\lambda_\tau=\pm 1/2}/dq^2$ are the helicity dependent differential decay rates.

3 Constraints on new Physics couplings

Using $b \to c\tau^-\bar{\nu}_\tau$ observables such as R_D, R_{D^*}, $P_\tau(D^*)$, $F_L(D^*)$, and $R(\Lambda_c)$, we perform a naive χ^2 analysis to constrain the NP SMEFT Wilson Coefficients (WCs), which serve as main constraints to the baryon decay. Additionally, we incorporate the $b \to s\ell\ell$ and $b \to s\nu\nu$ decay channels such as $\mathcal{B}(B^0 \to K^*\nu\nu)$, $\mathcal{B}(B \to K^+\nu\nu)$, $\mathcal{B}(B \to K^+\tau^+\tau^-)$ and $\mathcal{B}(B_s \to \tau^+\tau^-)$, to provide complementary constraints to the baryonic decay channel. Considering the 2d scenario the allowed parameter space is depicted in figure [1] i.e., considering two couplings at a time. The obtained best-fit values of SMEFT WCs are presented in the table [1].

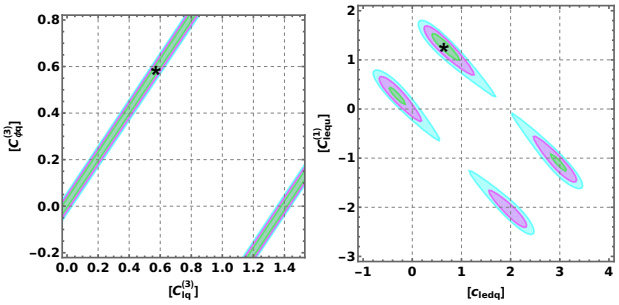

Figure 1. Allowed parameter space for the Scenario-I: $(C_{lq}^{(3)}, C_{\phi q}^{(3)})$ (Left) and Scenario:II $(C_{lequ}^{(1)}, C_{ledq})$ (Right) .

4 Analysis of $\Xi_b \to \Xi_c\tau^-\bar{\nu}_\tau$ Process

We focus on the various observables in our analysis. These observables are DBR, A_{FB}^{τ}, and R_{Ξ_b}. We investigate these observables in different 2d scenarios.

Figs. [2] and [3] depict the q^2 dependencies of the observables mentioned above, where we have incorporated the constraints from the $b \to c\tau^-\bar{\nu}_\tau$ observables. It is evident from figure [2] that in the presence of WCs $C_{lq}^{(3)}$ and $C_{\phi q}^{(3)}$, DBR and R_{Ξ_b} are quite in good agreement

SMEFT couplings	$b \to c\tau\nu_\tau$	$b \to s\tau^+\tau^-$	$b \to s\nu\bar{\nu}$
$(C_{lq}^{(3)}, C_{\phi q}^{(3)})$	(0.572, 0.587)	(-0.49, -0.078)	(0.08, 0.084)
$(C_{lq}^{(3)} = -C_{\phi q}^{(3)}, C_{lequ}^{(1)})$	(-0.007, -0.004)	—	—
$(C_{lq}^{(3)}, C_{lequ}^{(1)})$	(-0.014, -0.0038)	—	—
$(C_{lq}^{(3)} = -C_{\phi q}^{(3)}, C_{ledq})$	(-0.0051, -0.033)	—	—
$(C_{lq}^{(3)}, C_{ledq})$	(-0.0102, -0.033)	—	—
$(C_{lequ}^{(1)}, C_{ledq})$	(1.290, 0.650)	—	—

Table 1. Fit parameters corresponding to different 2d scenarios.

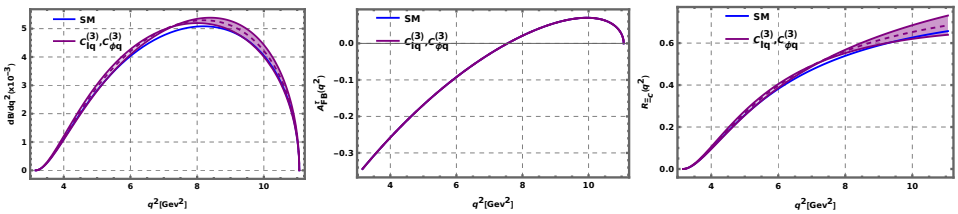

Figure 2. q^2 dependent DBR(Left), A_{FB}^{τ}(Middle) and R_{Ξ_b}(Right) in the presence of $C_{lq}^{(3)}$ and $C_{\phi q}^{(3)}$ WCs

with the SM prediction, however, a mild deviation can be seen in this observable. For the case of A_{FB}^{τ} the NP merges with SM prediction. Taking accounts WCs $C_{lequ}^{(1)}$, and C_{ledq} all observables show a significant deviation from their SM predictions. The DBR and the R_{Ξ_b} parameter show a significant deviation in the intermediate to high q^2 region, whereas the A_{FB} zero crossing point shifted in the presence of WCs $C_{lequ}^{(1)}$, and C_{ledq}. As mentioned earlier only $Q_{\ell q}^{(3)}$ and $Q_{\phi q}^{(3)}$ generate the $b \to s\ell\ell$ and $b \to s\nu\nu$ transition, hence can be a complementary channel to obtain bounds on corresponding WCs. Using the complementary bound on $C_{lq}^{(3)}$ and $C_{\phi q}^{(3)}$ WCs, q^2 dependent DBR , A_{FB}^{τ} and R_{Ξ_b} depicted in figures [4] and [5]. Figure [4] shows that there is a deviation in DBR and R_{Ξ_b} curve from the SM prediction while using the bounds on $C_{lq}^{(3)}$ and $C_{\phi q}^{(3)}$ obtained from $\mathcal{B}(B \to K^+\tau^+\tau^-)$ and $\mathcal{B}(B_s \to \tau^+\tau^-)$ process. Whereas for the case of bounds obtained from $\mathcal{B}(B^0 \to K^*\nu\nu)$, $\mathcal{B}(B \to K^+\nu\nu)$ process Figure [5] shows almost very tiny deviation from SM. For the A_{FB}^{τ} curve in the case of the complementary channel, it shows no deviation from SM in the presence of $C_{lq}^{(3)}$ and $C_{\phi q}^{(3)}$. The bound obtained from the $b \to s\tau^+\tau^-$ process incorporating these fit the DBR curves show significant deviation from SM prediction. Due to the difficulty in tau reconstruction, the upper limit on the branching fractions of the decays $B \to K^+\tau^+\tau^-$ and $B_s \to \tau^+\tau^-$ are far beyond the order of the SM prediction. Therefore, it has a larger parameter space compared to the $b \to s\nu\nu$ and $b \to c\ell\nu$ process.

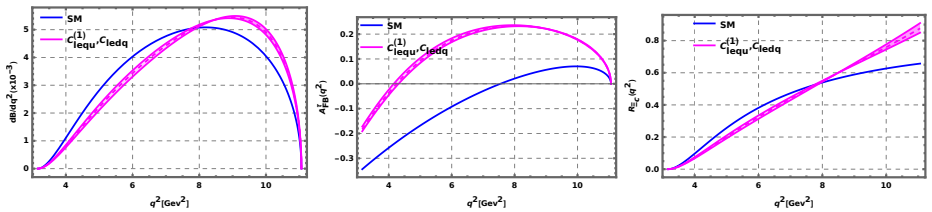

Figure 3. q^2 dependent DBR(Left),A^{τ}_{FB}(Middle) and R_{Ξ_b}(Right) in the presence of $(C^{(1)}_{lequ}, C_{ledq})$ WCs

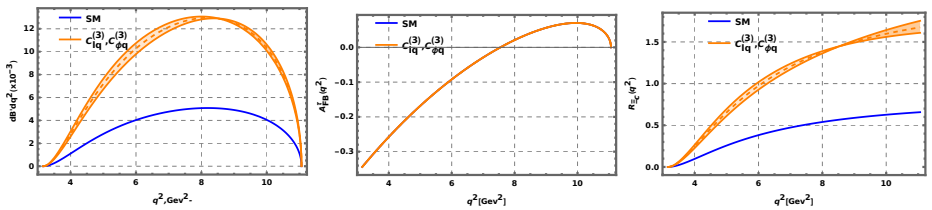

Figure 4. q^2 dependent DBR(Left), A^{τ}_{FB} (Middle) and R_{Ξ_b}(Right) in the presence of $(C^{(1)}_{lequ}, C_{ledq})$ WCs from $\mathcal{B}(B \to K^+\tau^+\tau^-)$ and $\mathcal{B}(B_s \to \tau^+\tau^-)$ Process.

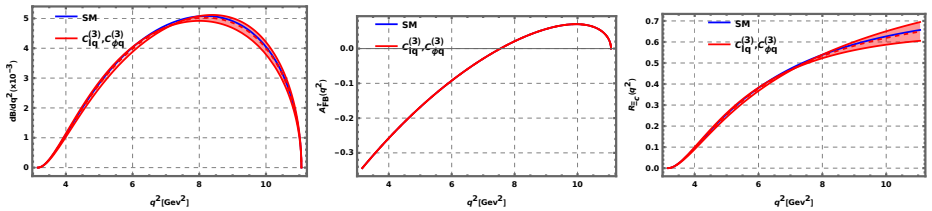

Figure 5. q^2 dependent DBR(Left) , A^{τ}_{FB} (Middle) and R_{Ξ_b}(Right) in the presence of $(C^{(1)}_{lequ}, C_{ledq})$ WCs from $\mathcal{B}(B_0 \to K^*\nu\nu)$, $\mathcal{B}(B \to K^+\nu\nu)$ process.

5 Conclusion

In this study, we figured out that there is a correlation between the $b \to c\ell\nu$ and $b \to s\nu\nu$ and $b \to s\ell\ell$ processes at the electroweak scale by SMEFT framework. we performed χ^2 fit for the Wilson coefficients and obtained the best-fit values for the various 2d combinations. Utilizing these outcomes, we investigated the semileptonic decay mode $\Xi_b \to \Xi_c\tau^-\bar{\nu}_\tau$ within the SM and beyond SM in the SMEFT framework. We presented various q^2 dependent observables in various NP scenarios. We found that the WCs $C^{(1)}_{lequ}$, and C_{ledq} show a significant impact on the q^2 dependent observable of $\Xi_b \to \Xi_c\tau^-\bar{\nu}_\tau$ decay and hence sensitive to NP effect.

References

[1] J. P. Lees *et al.* [BaBar], Measurement of an Excess of $\bar{B} \to D^{(*)}\tau^-\bar{\nu}_\tau$ Decays and Implications for Charged Higgs Bosons, Phys. Rev. D **88**, no.7, 072012 (2013) doi:10.1103/PhysRevD.88.072012 [arXiv:1303.0571 [hep-ex]].

[2] G. Caria *et al.* [Belle], Measurement of $\mathcal{R}(D)$ and $\mathcal{R}(D^*)$ with a semileptonic tagging method," Phys. Rev. Lett. **124**, no.16, 161803 (2020) doi:10.1103/PhysRevLett.124.161803 [arXiv:1910.05864 [hep-ex]].

[3] I. Adachi *et al.* [Belle-II], A test of lepton flavor universality with a measurement of $R(D^*)$ using hadronic B tagging at the Belle II experiment, [arXiv:2401.02840[hep-ex]].

[4] P. Asadi, M. R. Buckley and D. Shih, Asymmetry Observables and the Origin of $R_{D^{(*)}}$ Anomalies, Phys. Rev. D **99** (2019) no.3, 035015 doi:10.1103/PhysRevD.99.035015

[5] R. Aaij *et al.* [LHCb], Observation of the decay $\Lambda_b^0 \to \Lambda_c^+\tau^-\bar{\nu}_\tau$, Phys. Rev. Lett. **128** (2022) no.19, 191803 doi:10.1103/PhysRevLett.128.191803 .

[6] I. Ray and S. Nandi, JHEP **01** (2024), 022 doi:10.1007/JHEP01(2024)022 [arXiv:2305.11855 [hep-ph]]. I. Ray and S. Nandi,Test of new physics effects in $\overline{B} \to \left(D^{(*)}, \pi\right)\ell^-\bar{\nu}_\ell$ decays with heavy and light leptons,.JHEP **01**,022(2024). https://doi.org/10.1007/JHEP01(2024)022

[7] C. P. Haritha, K. Jain and B. Mawlong, Eur. Phys. J. C **83** (2023) no.2, 136. https://doi:10.1140/epjc/s10052-023-11282-8